Handling Qualities Assessment of Large Variable-RPM Multi-Rotor Aircraft for Urban Air Mobility

Matthew Bahr
Graduate Research Assistant

Michael McKay
Graduate Research Assistant

Robert Niemiec
Research Scientist

Farhan Gandhi
Redfern Professor and MOVE Director

Center for Mobility With Vertical Lift (MOVE)
Rensselaer Polytechnic Institute
Troy, NY, United States

ABSTRACT

Optimization-based control design techniques are applied to multicopters with variable-RPM rotors. The handling qualities and motor current requirements of a quadcopter, hexacopter, and octocopter with equal gross weights (1200 lb) and total disk areas (producing a 6 lb/ft^2 disk loading) are compared to one another in hover. For axes that rely on the rotor thrust (all except yaw), the increased inertia of the larger rotors on the quadcopter increase the current requirement, relative to vehicles with fewer, smaller rotors. Both the quadcopter and hexacopter have maximum current margin requirements (relative to hover) during a step command in longitudinal velocity. In yaw, rotor inertia is irrelevant, as the reaction torque of the motor is the same whether the rotor is accelerating or overcoming drag. This, combined with the octocopter's greater inertia as well as the fact that it requires 30% less current to drive its motors in hover, results in the octocopter requiring the greatest current margin, relative to hover conditions. To meet handling qualities requirements, the total weight of the motors of the octocopter and hexacopter is comparable at 15% weight fraction, but the quadcopter's motors are heavier, requiring 17% weight fraction. If the longitudinal and lateral axes were flown in ACAH mode, rather than TRC mode, the total motor weight of all configurations would be nearly identical, requiring about 14.6% weight fraction for motors (compared to 8-9% weight fraction from hover torque requirements).

NOTATION

Symbols

B	Motor Viscous Loss Coefficient
C_T	Rotor Thrust Coefficient
i	Motor Current
I_{rotor}	Rotor Inertia
K_e	Motor back-EMF Constant
K_t	Motor Torque Constant
L	Motor Inductance
M_u	Longitudinal Speed Stability Derivative
N_{rotors}	Number of Rotors
R	Rotor Radius
R_m	Motor Resistance
Q	Motor Torque
Q_A	Rotor Aerodynamic Torque
V	Motor Voltage
W_{eng}	Motor Weight
Ω	Rotor Speed
Ω_0	Collective Rotor Speed Mode
Ω_{1c}	Pitch Rotor Speed Mode
Ω_{1s}	Roll Rotor Speed Mode
Ω_d	Differential (Yaw) Rotor Speed Mode
$\dot{\Omega}$	Rotor Acceleration

Acronyms

ACAH	Attitude Command Attitude Hold
eVTOL	Electric Vertical Takeoff and Landing
OLOP	Open-Loop-Onset-Point
RMAC	Rensselaer Multicopter Analysis Code
RMS	Root Mean Square
TRC	Translational Rate Command
UAM	Urban Air Mobility
VTOL	Vertical Takeoff and Landing

INTRODUCTION

Electric Vertical Takeoff and Landing (eVTOL) aircraft are the centerpiece of Urban Air Mobility (UAM). The simplicity of electric drive systems has lowered the barriers to entry into this new space, resulting in a proliferation of new designs by manufacturers, both familiar and new. The simplest eVTOL design is the scaled-up multicopter, such as the Volocopter 2X or the Airbus CityAirbus, where lift and propulsive thrust are produced by several rotors distributed across the airframe. Other eVTOL archetypes include tiltrotors, such as the Bell Nexus or Joby S4, and "lift+cruise" vehicles, such as the Wisk Cora and the Aurora Flight Sciences PAV.

Presented at the VFS International 76th Annual Forum & Technology Display, Virginia Beach, VA, October 6–8, 2020.

Recently, considerable attention has been given to the handling qualities of eVTOL aircraft for UAM applications. Many of these multi-rotor eVTOL aircraft use fixed-pitch, variable-RPM rotors. While the simplicity of these rotors is attractive, their inability to rapidly generate thrust as rotor size (and inertia) increases can become a serious impediment. Recent studies by Walter et al. (Refs. 1,2) suggest that while 1'-4' diameter rotors would have satisfactory handling qualities, 6' and 8' diameter rotors (typical on manned-size eVTOL aircraft) would struggle to meet Level 1 handling qualities (due to saturation of motor power). However, the controllers used in Refs. 1,2 were not designed considering a complete set of handling qualities requirements. Other studies by Malpica and Withrow-Maser (Ref. 3) and Niemiec et al. (Ref. 4) compare the use of fixed-pitch, variable-RPM rotors to variable-pitch rotors on multi-rotor eVTOL aircraft.

The present study uses the optimization-based control design software CONDUIT® (Ref. 5) to develop controllers for 1200 lb gross weight multi-rotor eVTOL aircraft, where actuator activity is minimized while meeting a set of handling qualities based on ADS-33E-PRF (Ref. 6) specifications. These techniques have long been used on conventional VTOL aircraft (Ref. 7), and have also been applied to small eVTOL aircraft in recent years (Refs. 8–10). CONDUIT® is used to optimize inner loop and outer loop control laws on a 1200 lb quadcopter, hexacopter and octocopter, each having the same total disk area (and 6 lb/ft^2 disk loading). This allows a comparison of the three aircraft (ranging from the quadcopter with the largest, highest-inertia rotors to the octocopter with the smallest, lowest-inertia rotors) in terms of their ability to execute maneuvers and reject gusts. Rather than assume a particular actuator, and determine whether it is sufficient to meet handling qualities requirements, the motor current constraint is neglected. After optimizing for minimum actuator activity, the commanded current during different maneuvers and gust rejections will be used to determine the minimum motor size to meet handling qualities specifications.

PLATFORM

Aircraft Model

Three different aircraft configurations are considered, multicopters with four, six, and eight rotors. All three aircraft fly edge-first, shown in Fig. 1. In order to solve the six rigid-body equations of motion, six trim variables, comprised of multi-rotor speeds and the aircraft pitch and roll attitudes are required. The primary control modes are defined in multi-rotor coordinates (Ref. 11), and the multi-rotor coordinate transform (Eq. 1) provides the individual rotor speeds. The parameter Ψ_k represents the azimuthal rotor position, with 0° at the aft of the aircraft (Fig. 1). Ω_0 represents a uniform increase in individual rotor speed, which regulates the vertical axis. Ω_{1s} increases the rotor speed on the right of the aircraft and decreases the rotor speed on the left of the aircraft, providing roll control. Ω_{1c} provides pitch control by increasing the speed of the rear rotors while decreasing the speed of the front rotors, causing a nose-down moment. The differential mode, Ω_d, increases and decreases alternating rotor speed about the aircraft azimuth, resulting in a nose-right yaw moment (in steady-state operation). For the hexacopter and octocopter, there are additional, reactionless control modes, which are not utilized to solve the rigid body equations of motion.

$$\Omega_k = \Omega_0 + \Omega_{1s}\sin\Psi_k + \Omega_{1c}\cos\Psi_k + \Omega_d(-1)^{k-1} \qquad (1)$$

The three different aircraft all share disk loading of 6 psf and disk area equal to a single, 8 ft radius rotor. The shared aircraft parameters are shown in Table 1. The parameters that change across configurations are the number of rotors, rotor radius, and boom length, tabulated in Table 2. The boom length is chosen to maintain a $0.1R$ tip-to-tip separation.

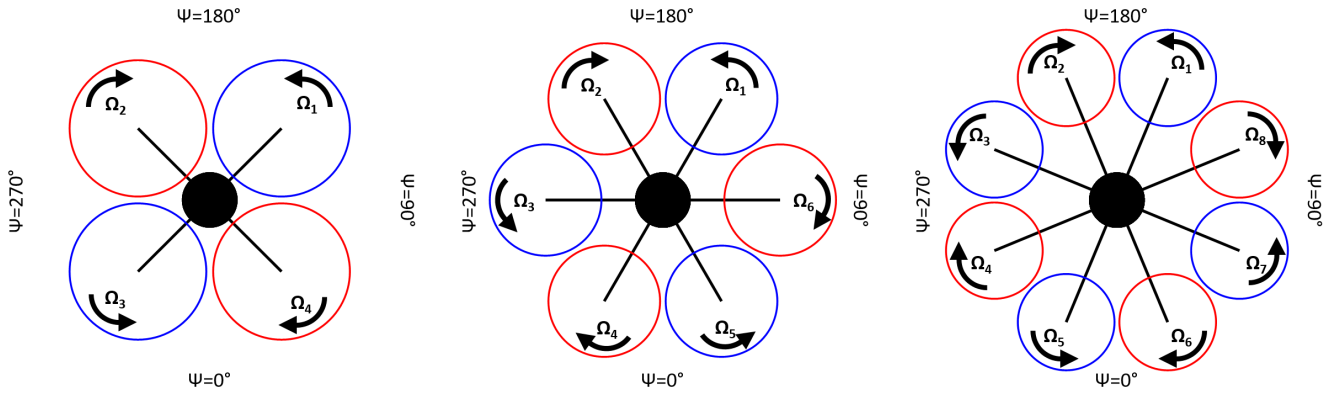

(a) Quadcopter (b) Hexacopter (c) Octocopter

Figure 1: Multicopter Configurations

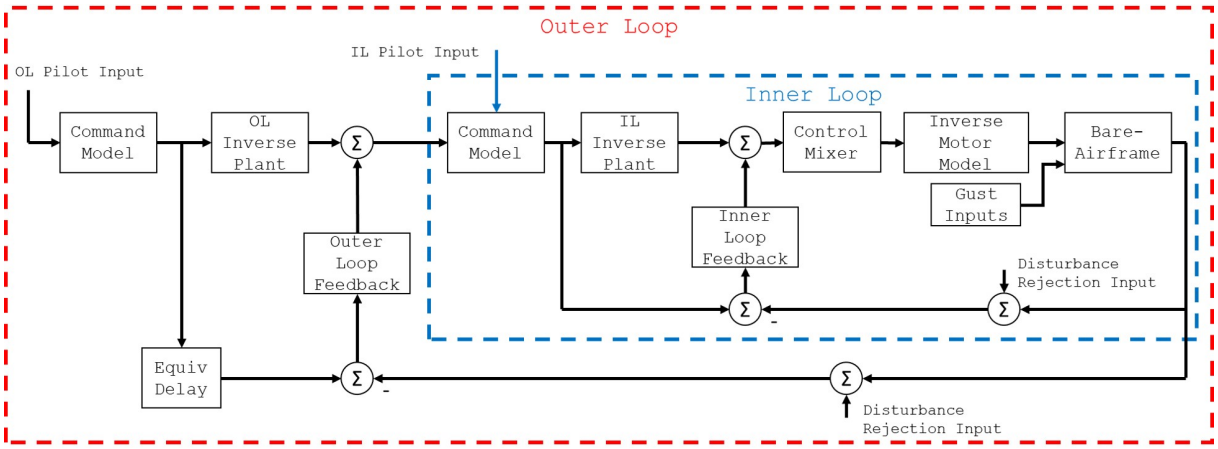

Figure 2: Control System Architecture

Table 1: Shared Aircraft Parameters

Parameter	Value
Gross Weight	1206 lb
Disk Loading	6 psf
Total Disk Area	64π ft^2
Rotor Root Pitch	21.5°
Rotor Twist	-10.4°
Tip Clearance	$0.1R$

Table 2: Varying Aircraft Parameters

Parameter	Quad	Hex	Oct
Rotor Radius [ft]	4	3.27	2.83
Boom Length [ft]	5.94	6.86	7.76
I_{xx} [slug ft^2]	344	370	401
I_{yy} [slug ft^2]	405	431	461
I_{zz} [slug ft^2]	667	719	781

Flight Dynamics Model

The rigid-body dynamics of each configuration are evaluated using the Rensselaer Multicopter Analysis Code (RMAC, Ref. 12). RMAC calculates the aircraft accelerations by summation of forces and moments at the aircraft center of gravity. Rotor forces and moments are calculated using blade element theory, with a 3x4 Peters-He finite-state dynamic wake model (Ref. 13). RMAC is used to identify a trim condition for the aircraft, as well as linearize the dynamics.

Motor Model

To properly evaluate the handling qualities, the dynamics of the electric DC motor must be modeled. The motor-rotor system model is laid out by Malpica and Withrow-Maser (Ref. 3). The rotor acceleration is given by

$$I_{\text{rotor}}\dot{\Omega} = K_t i - Q_A - B\Omega, \tag{2}$$

where $K_t i$ represents the motor torque constant, Q_A represents the aerodynamic torque, and $B\Omega$ represents viscous losses. The current of the motor is governed by Eq. 3,

$$L\frac{di}{dt} = V - K_e\Omega - R_m i, \tag{3}$$

where L is the motor inductance (usually very small), V is the applied voltage, $K_e\Omega$ represents the back-EMF of the motor ($K_e = K_t$ only if using SI units), and $R_m i$ represents the Ohmic losses across the motor.

If the inductance of the motor is completely neglected, the electrical dynamics settle instantaneously, and Eq. 3 can be solved for the motor current. Substituting the result into Eq. 2 and assuming the viscous losses are negligible yields

$$I_{\text{rotor}}\dot{\Omega} = \frac{K_t}{R_m}V - \frac{K_e^2}{R_m}\Omega - Q_A, \tag{4}$$

which is the governing equation for the rotor speed. Using a known rotor thrust, torque, speed, and assumed motor efficiency (95%), the motor parameters (K_t and R_m) can be calculated as in Ref. 3, and are tabulated in Table 3.

Table 3: Motor Parameters

	Quad	Hex	Oct
K_t [Nm/A][1]	1.18	0.79	0.59
R_m [mΩ]	47.5	47.5	47.5

[1] K_e [Vs/rad] is equivalent to K_t if using SI units

CONTROL OPTIMIZATION

A state space model linearized about a trim condition is utilized to design a control system. The control optimization suite CONDUIT® (Ref. 5) is used to optimize a controller for actuator effort, while meeting the specifications presented by ADS-33E-PRF (Ref. 6).

The explicit-model-following control architecture for the multicopters is illustrated in Fig. 2. The inner loop consists of attitude-command-attitude-hold (ACAH) response-type controllers on the longitudinal and lateral axes, along with a rate-command-direction-hold controller in yaw. Based on a desired attitude or yaw rate, the inner loop determines a desired

Table 4: CONDUIT® Inner Loop Hover Specifications

Specification	Axes
Hard Constraints	
EigLcG1	All
StbMgG1	Roll, Pitch, Yaw
NicMgG1	Roll, Pitch, Yaw
Soft Constraints	
BnwPiH1	Pitch
BnwRoH1	Roll
BnwYaH1	Yaw
CrsMnG2	Roll, Pitch, Yaw
DrbPiH1	Pitch
DrbRoH1	Roll
DrbYaH1	Yaw
DrpAvH1	Roll, Pitch, Yaw
EigDpG1	All
ModFoG1	All
OlpOpG1 (Pilot)	Roll, Pitch, Yaw
OlpOpG1 (Disturbance)	Roll, Pitch, Yaw
Summed Objectives	
RmsAcG1 (Pilot)	Roll, Pitch, Yaw
RmsAcG1 (Disturbance)	Roll, Pitch, Yaw
CrsLnG1	Roll, Pitch, Yaw

Table 5: CONDUIT® Outer Loop Hover Specifications

Specification	Axes
Hard Constraints	
EigLcG1	All
StbMgG1 (Inner Loop)	All
StbMgG1 (Outer Loop)	All
NicMgG1 (Inner Loop)	All
NicMgG1 (Outer Loop)	All
Soft Constraints	
CrsMnG2	All
DrbVxH1	Longitudinal
DrbVyH1	Lateral
DrbVzH1	Heave
DrpAvH1	All
FrqHeH1	Heave
EigDpG1	All
ModFoG1	All
OlpOpG1 (Pilot)	All
OlpOpG1 (Disturbance)	All
RisLoG1	Longitudinal & Lateral
Summed Objectives	
RmsAcG1 (Pilot)	All
RmsAcG1 (Disturbance)	All
CrsLnG1	All

speed for the rotors (in multi-rotor coordinates). After utilizing the multi-rotor coordinate transform (Eq. 1) to obtain the desired individual motor speeds, an open-loop controller (based on an inversion of a linearized Eq. 4) is used to determine the voltage delivered to each motor. The specifications used for the inner loop controller are listed in Table 4.

The outer loop consists of translational rate command (TRC) controllers in the longitudinal, lateral, and vertical axes. For the longitudinal and lateral axes, the outer loop determines a desired pitch and roll attitude, which commands the ACAH controllers in the inner loop. For the vertical axis, the outer loop determines a desired mean rotor speed, which is fed directly to the control mixer. The outer loop specifications are listed in Table 5.

Included in both the inner and outer loops is an Open-Loop-Onset-Point (OLOP) specification. This specification indicates whether a vehicle is susceptible to pilot-induced or limit-cycle oscillations due to actuator rate saturation. In the case of a variable-RPM multicopter, the key limitation is the deliverable current to the motor, which corresponds to a limit in $\dot{\Omega}$. Thus, for the OLOP specifications, a maximum current is assumed using a design parameter, K (in terms of the hover current, the maximum current is $K \times i_{\text{hover}}$). From Eqn. 2 (neglecting viscous losses), this motor will have a maximum $\dot{\Omega}$ of

$$\dot{\Omega}_{\max} = \frac{K_t (K-1) i_{\text{hover}}}{I_{\text{rotor}}}, \tag{5}$$

which is used for the evaluation of the OLOP specification. By increasing or reducing K until the OLOP specification is on the Level 1/2 boundary, a minimum motor current margin can be identified.

Table 6: Hover Performance

	Quad	Hex	Oct
Ω_0 [rad/s]	114	139	161
Tip Speed [ft/s]	455	455	455
Rotor Thrust [lb]	302	201	151
Rotor Torque [ft-lb]	131	71.1	46.2
Motor Power [each, hp]	28.4	18.9	14.2
Motor Current [each, A]	150	122	106
Motor Voltage [V]	141	115	100
Total Vehicle Power [hp]	113	113	113
Motor Weight Fraction[1]	9.4%	8.6%	8.1%

[1]Represents Weight Fraction from Hover Torque Requirement Only, Calculated from Eq. 6 on Page 8

RESULTS

Hover Trim and Performance

The hover performance for all configurations is tabulated in Table 6. Naturally, in hover, only collective RPM is required, as there are no external moments to balance (the vehicle C.G. is assumed to be located at the geometric center of the aircraft). As the rotors of the three vehicles all have the same pitch, solidity, and airfoil distribution, they have a common C_T. This, combined with the fact that all three vehicles have identical disk loading, results in the configurations having the

same vehicle power and rotor tip speed of 455 ft/s. Both the nominal voltage and individual motor current scale with $N_{\text{rotors}}^{-1/2}$, which suggests that having more rotors will generally increase vehicle current requirements (scales with $N_{\text{rotors}}^{1/2}$), suggesting that electrical losses (not modeled in this study) may be greater on an octocopter than a quadcopter. To meet hover torque requirements, the quadcopter requires the largest motor weight fraction (9.4%), with the hexacopter (8.6%) and octocopter (8.1%) requiring less.

Inner Loop Performance

CONDUIT® was able to achieve Level 1 handling qualities specifications for all three multicopters. The inner loop handling qualities results are tabulated in Table 7. As expected, considering the similarity in the vehicle dynamics, the quadcopter, hexacopter, and octocopter achieve similar levels of performance in nearly all of the handing qualities specifications. The only notable exception is the OLOP specification in yaw, which generally gets worse as the number of rotors increases.

The values reported in Table 7 represent a case where the motor current margin is equal to the current required to hover ($K = 2$). This results in overperformance in the OLOP specifications, suggesting that motor weight reduction is possible without violating any of the handling qualties specifications. The quadcopter and hexacopter reach the Level 1/2 boundary of the OLOP specification with a 53% ($K = 1.53$) motor current margin, limited by roll disturbance input. The octocopter reaches the Level 1/2 boundary at 62% ($K = 1.62$) current margin, limited by a piloted yaw rate input.

For the actuator RMS objective functions in pitch, there are multiple effects to consider. Specifically, the reduced inertia of the rotors reduces the actuator effort required as the rotor radius decreases. In evaluating RMS, the raw inputs are normalized by a reference value derived from the hover voltage (which is lower as more rotors are added). These two effects largely cancel out in pitch, and the RMS specifications are similar.

However, in yaw, the rotor inertia has no effect on the actuator activity level. This is because the reaction torque experienced by the aircraft is directly dependent on the motor torque/current. Whether that torque is used to accelerate the rotor, or overcome aerodynamic drag is irrelevant—the effect on the aircraft is the same. However, the normalization still occurs, which results in higher RMS as the number of rotors increases.

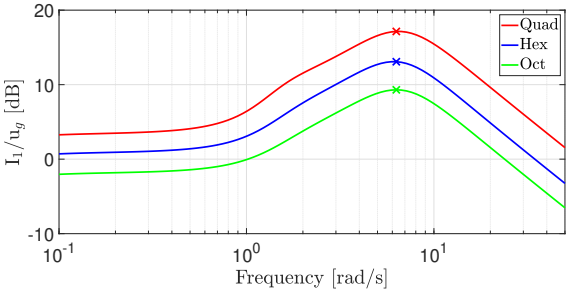

Figure 3: Frequency Response of Longitudinal Gust to Motor 1 Current

Inner Loop Time Simulations As another means of determining the current requirements for maneuver, several time-domain simulations were run. To examine the behavior under piloted inputs, doublet and step commands were given to the inner loop. For disturbance analysis, 1-cosine gusts (Ref. 14) were applied. The gust duration is determined by the frequency which maximizes the motor current due to a gust in-

Table 7: Inner Loop Handling Qualities Specifications

Parameter	Unit	Pitch			Yaw		
		Quad	Hex	Oct	Quad	Hex	Oct
Stability Gain Margin[1]	dB	13	14	16			
Stability Phase Margin	deg	49	45	45	109	106	101
Disturbance Rejection Bandwidth	rad/s	1.16	1.27	1.34	0.97	0.97	0.98
Disturbance Rejection Peak	dB	3.35	3.66	3.71	0.27	0.24	0.22
Bandwidth	rad/s	2.49	2.5	2.5	1.4	1.4	1.4
Phase Delay	ms	84	86	80	2.1	2.0	2.0
Crossover Frequency	rad/s	5.0	5.0	5.3	5.0	5.0	5.0
Command Model Following	–	49	42	30	0.06	0.05	0.06
OLOP Magnitude (Pilot)[2]	dB						-3.4
OLOP Phase (Pilot)[2]	deg						-69
OLOP Magnitude (Disturbance)	dB	-4.3	-5.7	-6.1	0.30	1.75	3.0
OLOP Phase (Disturbance)	deg	-137	-142	-142	-72	-80	-88
Actuator RMS (Pilot)	–	0.029	0.026	0.025	0.094	0.13	0.17
Actuator RMS (Disturbance)	–	0.11	0.13	0.14	0.78	1.19	1.62

[1]Blank entry indicates no 180° crossing in relevant frequency range
[2]Blank entry indicates that rate limit not reached at relevant frequency range

put, shown on the Bode plot in Fig. 3. The three configurations share a frequency (6.3 rad/s, 1 second period) which maximizes motor current. The magnitude of piloted and gust inputs is equal to the maximum input used to evaluate the OLOP specification. For both types of inputs, the motor current response of all three vehicles were examined.

Longitudinal Axis The longitudinal and lateral axes are qualitatively similar on multicopters, due to the symmetry of the configuration. The only difference between the two is that the pitch inertia is slightly greater than the roll inertia. Thus, the longitudinal axis will require greater effort to control, and is presented here.

A 10° pitch doublet is used as pilot input and is plotted along with the filtered commands and the closed-loop response of the vehicle in Fig. 4a. All three vehicles respond similarly, as expected, since they were all tuned to the same closed-loop requirements. The octocopter follows the command with the least error, followed by the hexacopter and quadcopter.

Figure 4b shows the current change required by the most longitudinally extreme rotors on the quadcopter, hexacopter, and octocopter (Motor 1 for all three, Fig. 1). The current is normalized by the current required to hover in Table 6, this normalization represents a relative current margin required to execute the maneuver. All three curves are characterized by large current spikes when the pitch command goes through a step change. When this occurs, the desired motor speeds change rapidly, requiring a surge in motor torque/current. The quadcopter requires the greatest margin (33%), followed by the hexacopter (32%) and octocopter (28%), as the smaller rotors have less rotational inertia to overcome.

The response of the vehicles to a 20 knot 1-cosine (Ref. 14) longitudinal gust (applied as a tailwind) is shown in Fig. 5. As the aircraft experience a tailwind, they initially pitch nose-down (due to a positive M_u), and the feedback controller reacts to stabilize the vehicle and return it to a nose-level condition. The maximum nose-down deflection is around 5 degrees, and is slightly reduced as the number of rotors increases. The current delivered to the front-right rotor is plotted in Fig. 5b, again normalized by the hover current of each individual aircraft. Naturally, the current supplied to this rotor is positive initially, as the aircraft tries to produce a nose-up moment to counteract the effect of the gust. The quadcopter requires the greatest current margin of all three configurations, due to the greater inertia of its rotors.

Rejecting a 20 knot gust requires less current than following the 10° doublet command for all configurations. The quadcopter requires 30% current margin to reject the gust, while the hexacopter and octocopter require 24% and 18% current margin, respectively. The quadcopter has comparable current margin when rejecting the gust or following the doublet command, requiring only 3% less than the doublet. This difference is more pronounced as the number of rotors increases, with the hexacopter and octocopter having an 8% and 10% lower current requirement for gust rejection, respectively.

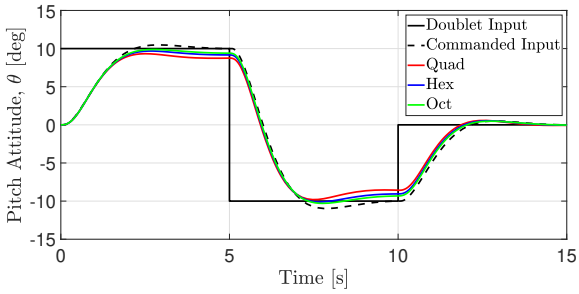

(a) Command Input and Vehicle Response

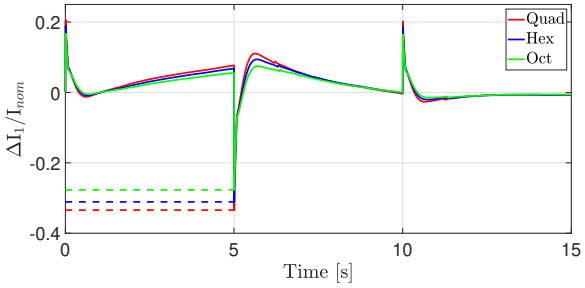

(b) Motor 1 Normalized Current Response

Figure 4: Pitch Response to a Doublet Command

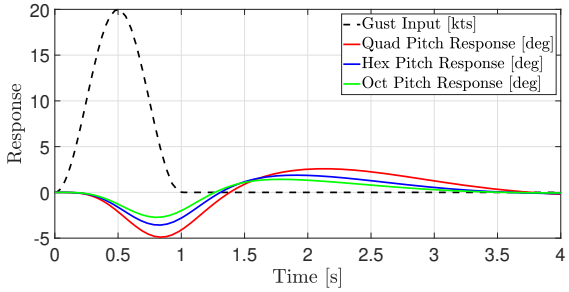

(a) Gust Input and Pitch Response

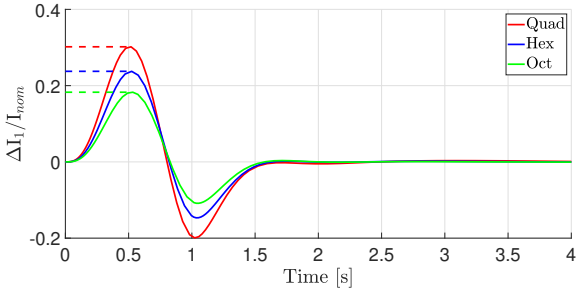

(b) Motor 1 Normalized Current Response

Figure 5: Inner Loop Response to Longitudinal Gust

Yaw Axis To examine the vehicle response to a piloted input in yaw rate, a 20°/second step command was issued to all three vehicles (Fig. 6a). All three vehicles respond identically, as expected, following the first-order command model well.

The current (normalized by the hover current of each individual aircraft) required by the front-right rotor to follow the yaw step is plotted in Fig. 6b. At the beginning of the simulation, the desired yaw acceleration is very high, which will require a large surge in the motor torque/current. Importantly, unlike the other axes, the vehicle does not rely on the rotor speed for yaw moment, so the primary advantage of the octocopter over the quadcopter and hexacopter is gone. In fact, the octocopter requires the greatest current margin of all three configurations, requiring 111% of the hover current margin. The quadcopter and hexacopter require significantly less current margin in this axis, requiring 67% hover and 89% hover current margin, respectively. The octocopter requires the greatest current margin due to it having the greatest yaw inertia (Table 2), which requires more torque to accelerate.

Outer Loop Performance

CONDUIT® was also able to achieve Level 1 handling qualities for all three configurations in the outer loop and are tabulated in Table 8. As was the case for pitch in the inner loop, all of the aircraft achieve the same level of performance. With both the longitudinal and vertical axes relying on motor speed change, as the rotors become smaller, there is a decrease in actuator RMS for piloted and disturbance inputs.

Longitudinal Axis The aircraft and motor 1 current response to a 10 knot longitudinal velocity step command is shown in Figs. 7a and 7b, respectively. The response of all three configurations is nearly identical, as expected. Similar to pitch in ACAH mode, as the number of rotors increases, the required current to each motor decreases. For all three configurations, the required current is significantly greater for this input than the 10° doublet command. This increase in current is due to a higher pitch command model frequency, which is necessary to meet minimum phase margin requirements in the outer loop.

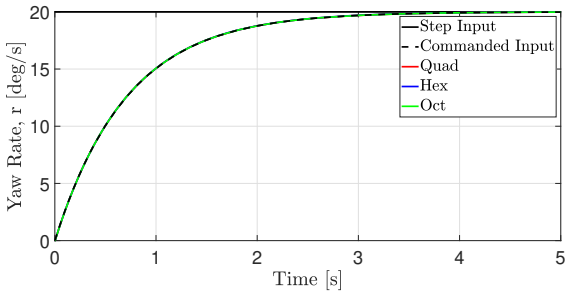

(a) Command Input and Vehicle Response

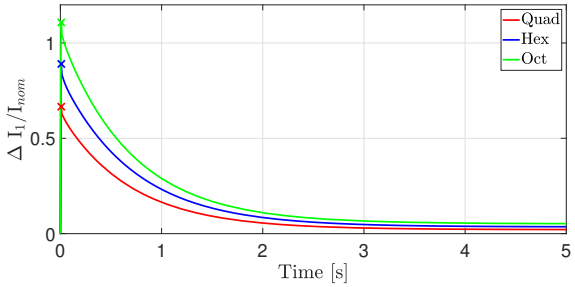

(b) Motor 1 Normalized Current Response

Figure 6: Yaw Response to a Step Command

Table 8: Outer Loop Handling Qualities Specifications

Parameter	Unit	Longitudinal			Heave		
		Quad	Hex	Oct	Quad	Hex	Oct
Stability Gain Margin[1]	dB	8.4	8.8	9.1			
Stability Phase Margin	deg	55	52	51	87	87	87
Disturbance Rejection Bandwidth	rad/s	0.60	0.60	0.60	0.5	0.5	0.5
Disturbance Rejection Peak	dB	5.0	4.9	4.9	0.63	0.63	0.62
Crossover Frequency	rad/s	1	1	1	1.05	1.05	1.05
Command Model Following	–	6.1	3.0	1.8	0.01	0.01	0.01
Heave Mode Pole	rad/s				0.2	0.2	0.2
Heave Mode Time Delay	ms				89	89	87
Rise Time	s	5	4.9	4.9			
OLOP Magnitude (Pilot)[2]	dB	-31	-76				
OLOP Phase (Pilot)[2]	deg	-280	-328				
OLOP Magnitude (Disturbance)	dB	-5.0	-6.9	-8.8	-3.8	-5.1	-6.2
OLOP Phase (Disturbance)	deg	-155	-167	-178	-98	-99	-101
Actuator RMS (Pilot)	–	0.15	0.14	0.13	0.10	0.080	0.072
Actuator RMS (Disturbance)	–	0.70	0.64	0.57	0.96	0.79	0.72

[1]Blank entry indicates no 180° crossing in relevant frequency range
[2]Blank entry indicates that rate limit not reached at relevant frequency range

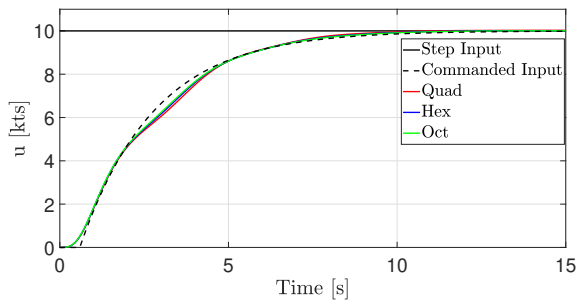

(a) Command and Vehicle Response

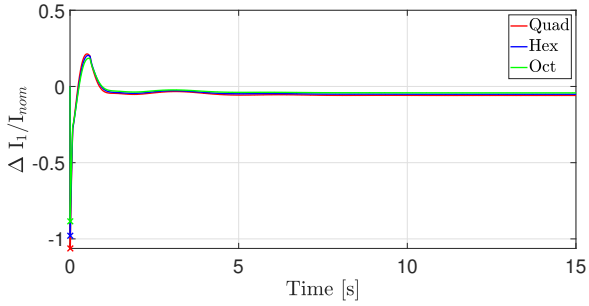

(b) Motor 1 Normalized Current Response

Figure 7: Outer Loop Longitudinal Velocity Step Response

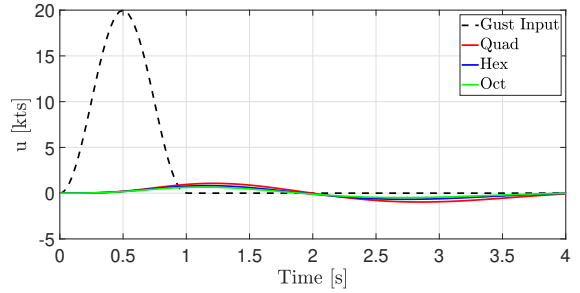

(a) Gust Input and Response

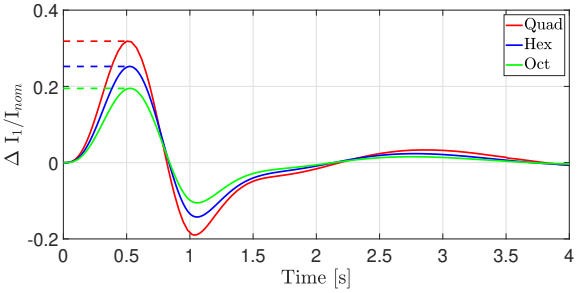

(b) Motor 1 Normalized Current Response

Figure 8: Outer Loop Response to Longitudinal Gust

The quadcopter requires 106% of its hovering current, and the hexacopter and octocopter require slightly less current margin, needing 98% and 88% of hover current, respectively.

A 1-cosine gust with a 1 second duration (dashed black line in Fig. 8a) was applied to all three configurations. For all three aircraft, the tailwind causes the aircraft to drift forward, and the feedback controller returns it to a steady hover within 4 seconds after the end of the gust. The current (Fig. 8b) follows a similar trend to the ACAH response-type, with the quadcopter requiring about 32% current margin to reject the gust, while the hexacopter and octocopter require 25% and 19% current margin, respectively. This current margin is similar to the inner loop gust rejection requirements, and is much less than is required during the step command in velocity.

Heave Axis A 1000 ft/min climb rate is commanded to all three multicopters in Fig. 9a. As expected from the identical handling qualities specifications, all three vehicles follow the same trajectory. Since heave control relies on the rotor thrust (and thus speed), similar trends with the longitudinal axis are observed in the motor current, plotted in Fig. 9b. The quadcopter requires the greatest current margin (71%), while the hexacopter (58%) and octocopter (52%) require less.

Similar to the longitudinal axis, a 20 knot magnitude 1-cosine downdraft was applied to the vertical axis of all three configurations. The frequency for this gust (0.1 rad/s, 63 second duration) was chosen to maximize the motor current. All three aircraft have the same response to the vertical gust, reaching a 1 knot peak magnitude heave response shown in Fig. 10a. All three configurations also utilize the same normalized current to reject the gust, requiring 25% of hover current shown in Fig. 10b. All three vehicles behave identically due to the quasi-steady behavior of the gust.

The effect of the rotor inertia can be observed for higher-frequency gusts. A 20 knot magnitude, 1.26 second duration (5 rad/s frequency) gust is applied to the vertical axis of all three configurations in Fig. 11a, while the required motor current is shown in Fig. 11b. All three configurations respond identically to the gust, reaching a descent heave rate of nearly 2 knots. The quadcopter requires the highest current margin, needing 19% hover current, while the hexacopter and octocopter require 17% and 16% hover current, respectively.

Motor Weight

An estimation for motor weight can be made based on the peak current across all maneuvers for each configuration. The peak motor torque is determined by the product of the motor torque constant and peak current. This peak motor torque can then be related to a motor weight using Eq. 6 (Ref. 15), with torque in ft-lb and resulting motor weight in lb.

$$W_{eng} = 0.5382 Q^{0.8129} \tag{6}$$

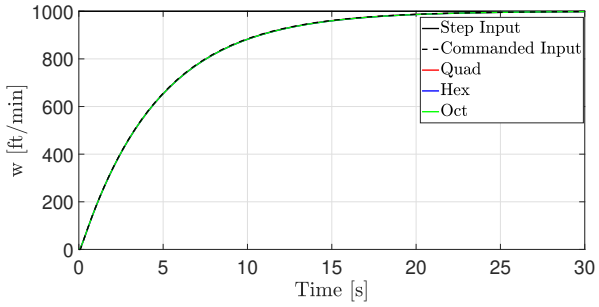

(a) Command and Vehicle Response

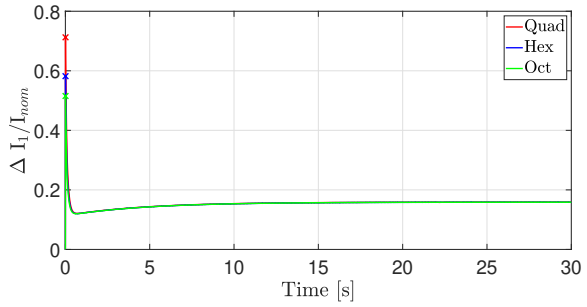

(b) Motor 1 Normalized Current Response

Figure 9: Step Command in Heave

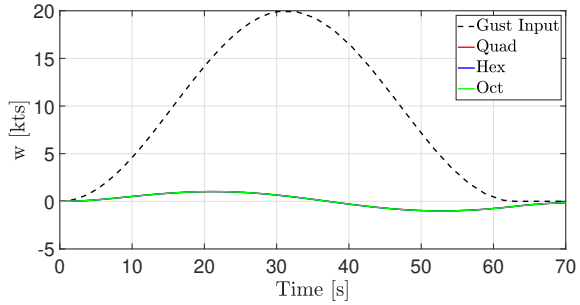

(a) Gust Input and Response

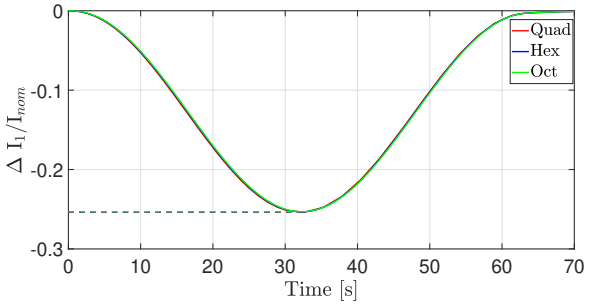

(b) Motor 1 Normalized Current Response

Figure 10: Outer Loop Response to Heave Gust (0.1 rad/s Frequency)

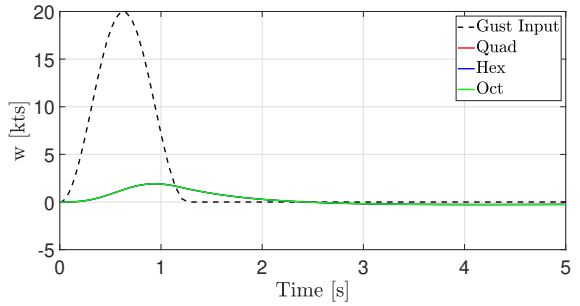

(a) Gust Input and Response

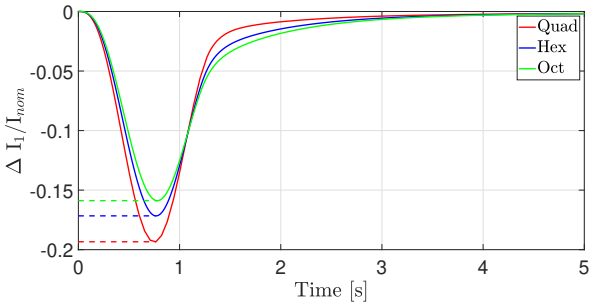

(b) Motor 1 Normalized Current Response

Figure 11: Outer Loop Response to Heave Gust (5 rad/s Frequency)

The limiting case for each configuration and the resulting motor weight is summarized in Table 9. Both the quadcopter and hexacopter are limited by a longitudinal velocity command, while the octocopter is limited by a yaw rate command. The quadcopter requires individual motors that are more than 20 lb heavier than the hexacopter or octocopter. The hexacopter and octocopter have roughly the same motor weight fraction (of about 15%), while the quadcopter is about 17%. Compared to hover requirements (Table 6), the quadcopter requires an additional 7.5% motor weight fraction to meet handling qualities requirements, while the hexacopter and octocopter require an additional 6.4% and 6.7%, respectively.

If the longitudinal and lateral axes are flown exclusively in ACAH mode, the limiting cases for the quadcopter and hexacopter become heave and yaw rate step commands, respectively. The current margin and motor weight are summarized in Table 10. The only vehicle to see any substantial reduction in the required motor weight is the quadcopter, which is now similar to the hexacopter and octocopter. The latter two configurations may further benefit from the introduction of rotor cant, which can reduce the current required to yaw the vehicle by reorienting rotor thrust to produce a direct yaw moment (Ref. 4). However, this comes at the cost of increasing the rotor thrust needed to regulate the other axes, so the quadcopter cannot benefit in the same way.

Table 9: Maximum Current & Motor Weight, With Outer-Loop TRC

Configuration	Maneuver	Maximum Current (A)	Maximum Torque (ft-lb)	Motor Weight (lb, each)	Weight Fraction (%)
Quadcopter	Longitudinal Velocity Step	310	270	50.9	16.9
Hexacopter	Longitudinal Velocity Step	243	141	30.1	15.0
Octocopter	Yaw Rate Step	224	97.5	22.3	14.8

Table 10: Maximum Current & Motor Weight, Without Outer-Loop TRC

Configuration	Maneuver	Maximum Current (A)	Maximum Torque (ft-lb)	Motor Weight (lb, each)	Weight Fraction (%)
Quadcopter	Heave Step	257	224	43.8	14.5
Hexacopter	Yaw Rate Step	232	135	29.0	14.4
Octocopter	Yaw Rate Step	224	97.5	22.3	14.8

CONCLUSIONS

Optimization-based control design techniques were applied to a 1200 lb gross weight quadcopter, hexacopter, and octocopter with variable-RPM rotors, and the handling qualities and relative motor requirements were compared in hover at 6 lb/ft^2 disk loading. When held to the same handling qualities requirements, all three configurations follow commands and reject disturbances identically to one another.

In axes that are regulated by rotor thrust, namely, pitch, roll, and heave, configurations with more rotors required less current margin than similarly sized vehicles with fewer, larger rotors. This is due to the fact that, in order to change thrust on a variable-RPM vehicle, the rotor's inertia must be overcome. Both the quadcopter and hexacopter were limited in axes that are regulated by rotor thrust. A step command in longitudinal velocity required 106% and 98% of hover current for the quadcopter and hexacopter, respectively.

In yaw, the dependence is directly on motor current, as the motor reaction torque (regardless of whether the motor is overcoming aerodynamic drag or accelerating the rotor) is what controls the aircraft. Because the octocopter has slightly more inertia in yaw (longer booms are needed to maintain rotor tip clearance), the octocopter requires the greatest current (111% of the hover current) of all three configurations to follow a yaw rate step command.

By utilizing the relationship between motor torque and weight, an estimate for motor weight necessary to maneuver the aircraft to ADS-33E-PRF (Ref. 6) standards was obtained. The limiting cases for the quadcopter and hexacopter were a step command in longitudinal velocity, while the yaw rate step command was limiting for the octocopter. If only hover torque requirements are considered, the motors represent an 8-9% weight fraction. When handling qualities requirements (with TRC) are considered, the motors represent a 15-17% weight fraction. To meet handling qualities requirements, the quadcopter's motors collectively weigh 23 lb (approximately 2% of the aircraft weight) more than the motors of the hexacopter or octocopter.

ACKNOWLEDGMENTS

This work is carried out at Rensselaer Polytechnic Institute under the Army/Navy/NASA Vertical Lift Research Center of Excellence (VLRCOE) Program, grant number W911W61120012, with Dr. Mahendra Bhagwat as Technical Monitor. The authors would also like to acknowledge the Army Research Office for funding Mr. McKay through the National Defense Science and Engineering Graduate Fellowship.

REFERENCES

1. Walter, A., McKay, M., Niemiec, R., Gandhi, F., and Jaran, C., "An Assessment of Heave Response Dynamics for Electrically Driven Rotors of Increasing Diameter," 8th Biennial Autonomous VTOL Technical Meeting 6th Annual Electric VTOL Symposium, Mesa, AZ, January 29–31, 2019.

2. Walter, A., McKay, M., Niemiec, R., Gandhi, F., and Ivler, C., "Handling Qualities Based Assessment of Scalability for Variable-RPM Electric Multi-Rotor Aircraft," VFS 75th Annual Forum, Philadelphia, PA, May 13–16, 2019.

3. Malpica, C., and Withrow-Maser, S., "Handling Qualities Analysis of Blade Pitch and Rotor Speed Controlled eVTOL Quadrotor Concepts for Urban Air Mobility," VFS Inernational Powered Lift Conference 2020, San Jose, CA, January 21–23, 2020.

4. Niemiec, R., Gandhi, F., Lopez, M., and Tischler, M., "System Identification and Handling Qualities Perdictions of an eVTOL Urban Air Mobility Aircraft Using Modern Flight Control Methods," VFS 76th Annual Forum, Virginia Beach, VA, October 6–8, 2020.

5. Tischler, M., Berger, T., Ivler, C., Mohammadreza, M. H., Cheung, K. K., and Soong, J. Y., "Practical Methods for Aircraft and Rotorcraft Flight Control Design: An Optimization-Based Approach," AIAA Education Series, Reston, VA, 2017.

6. "Aeronautical Design Standard, Performance Specification, Handling Qualities Requirements for Military Rotorcraft," Technical Report ADS-33E-PRF, March 2000.

7. Ivler, C., and Tischler, M., "Case Studies of System Identification Modeling for Flight Control Design," *Journal of the American Helicopter Society*, Vol. 58, (1), January 2013, pp. 1–16.

8. Wei, W., Tischler, M. B., and Cohen, K., "System Identification and Controller Optimization of a Quadrotor Unmanned Aerial Vehicle in Hover," *Journal of the American Helicopter Society*, Vol. 62, (4), October 2017, pp. 1–9.

9. Cheung, K., Wagster, J., Tischler, M., Ivler, C., Berrios, M., Berger, T., Juhasz, O., Tobias, E., Goerzen, C., Barone, P., Sanders, F., Lopez, M., and Lehmann, R., "An Overview of the U.S. Army Aviation Development Directorate Quadrotor Guidance, Navigation, and Control Project," , May 9–11, 2017.

10. Lopez, M., Tischler, M., Juhasz, O., Gong, A., Sanders, F., Soong, J., and Nadell, S., "Flight Test Comparison of Gust Rejection Capability for Various Multirotor Configurations," VFS 75th Annual Forum, Philadelphia, PA, May 13–16, 2019.

11. Niemiec, R., and Gandhi, F., "Multi-rotor Coordinate Transforms for Orthogonal Primary and Redundant Control Modes for Regular Hexacopters and Octocopters," 42nd Annual European Rotorcraft Forum, Lille, France, September 5–8, 2016.

12. Niemiec, R., and Gandhi, F., "Development and Validation of the Rensselaer Multicopter Analysis Code (RMAC): A Physics-Based Comprehensive Modeling Tool," Vertical Flight Society 75th Annual Forum, Philadelphia, PA, May 2019.

13. Peters, D., Boyd, D., and He, C. J., "Finite-State Induced-Flow Model for Rotors in Hover and Forward Flight," *Journal of the American Helicopter Society*, Vol. 34, (4), 1989, pp. 5–17.

14. Berrios, M., Berger, T., Tischler, M., Juhasz, O., and Sanders, F., "Hover Flight Control Design for UAS Using Performance-based Disturbance Rejection Requirements," AHS 73rd Annual Forum, Fort Worth, TX, May 9–11, 2017.

15. Johnson, W., "NDARC - NASA Design and Analysis of Rotorcraft," Technical Report NASA TP 218751, April 2015.